

Incomplete Caspase 3 Activation and Mitigation of Apoptosis in Hibernating Ground Squirrels, *Spermophilus lateralis*^{*}

Michael D. Treat

Anthony J. Marlon

Frank van Breukelen[†]

School of Life Sciences, University of Nevada, Las Vegas,
Nevada 89154

Accepted 9/19/2022; Electronically Published 1/26/2023

Online enhancement: appendix.

ABSTRACT

Hibernating golden-mantled ground squirrels, *Spermophilus* [*Callospermophilus*] *lateralis*, tolerate proapoptotic conditions, such as low body temperature, anorexia, acidosis, and ischemia/reperfusion. Avoiding widespread apoptosis is critical for hibernator survival. Caspase 3, the key executioner of apoptosis, cleaves a majority of apoptotic targets. Under proapoptotic conditions, inactive procaspase 3 (32 kDa) is activated when cleaved into 17- and 12-kDa fragments (p32, p17, and p12, respectively). Caspase 3 activation results in extreme enzymatic activation. Activity increases >10,000-fold followed by apoptotic execution. Is widespread apoptosis occurring during the proapoptotic hibernation season? Western blots showed p17 increased ~2-fold during hibernation, indicating caspase 3 activation. However, in vitro caspase 3 activity assays found no extreme increases in activity. Downstream caspase 3 targets ICAD (inhibitor of caspase-activated deoxyribonuclease) and PARP (poly (ADP-ribose) polymerase) did not experience elevated cleavage during hibernation, which is inconsistent with caspase 3 activation. TUNEL (terminal deoxynucleotidyl transferase-mediated deoxyuridine triphosphate nick-end labeling) assays from multiple tissues found only 0.001%–0.009% of cells were TUNEL positive during winter, indicating negligible apoptosis during hibernation. Typically, caspase 3 activation gen-

erates a strong commitment toward apoptosis. We found that despite a ~2-fold increase in active caspase 3, hibernators experience no downstream caspase 3 activity or widespread apoptosis. A systems-level approach suggests an incomplete signaling cascade wherein some caspase 3 activation during hibernation does not necessarily lead to bona fide apoptosis.

Keywords: proapoptotic, DEVD-AMC, p17 fragment, poly (ADP-ribose) polymerase (PARP), inhibitor of caspase-activated deoxyribonuclease (ICAD), terminal deoxynucleotidyl transferase-mediated deoxyuridine triphosphate nick-end labeling (TUNEL).

Introduction

Presumably in response to low environmental temperatures and limited resources, many mammals hibernate (van Breukelen and Martin 2015; Andrews 2019; Geiser 2021). During hibernation, ground squirrels enter torpor wherein oxygen consumption may be as low as 1/100th of active rates and body temperature (T_b) approaches ambient temperature (T_a) to as low as -2.9°C (Barnes 1989; Wang and Lee 1996). The hibernation phenotype results in ~90% energetic savings across the season. However, hibernation is not static. Instead, extended bouts of torpor (up to ~3 wk depending on time of season, species, and T_a) are interrupted by brief 12–20-h bouts of euthermia known as interbout arousals. This cycling between torpid and aroused states may be repeated 15 times or more per season (van Breukelen and Martin 2002a). The hibernation season represents a severely energy-limited state for ground squirrels, as they survive solely on endogenously stored resources (mainly fat). Therefore, reducing energetically demanding processes (e.g., transcription, translation, protein metabolism, cell division, apoptosis) is important during the hibernation season (van Breukelen and Martin 2002a).

While it may be tempting to speculate that ground squirrels are highly adapted to hibernate, as many as 40% of adult squirrels die each winter in the wild (Sherman and Morton 1984). The reason for this high mortality rate is still unknown, although physiological mismatches associated with heterothermy may contribute (van Breukelen et al. 2008). For instance, each time ground squirrels enter torpor, they experience a reduction in heart rate

*This paper included in the Focused Collection “Time-Out for Survival: Hibernation and Daily Torpor in Field and Lab Studies” is based on research presented at the 2021 16th International Hibernation Symposium (IHS) organized by Guest Handling Editors Rob Henning, Roelof Hut, and Hjalmar Bouma.

†Corresponding author; email: frank.vanbreukelen@unlv.edu.

that precedes appreciable changes in T_b (e.g., there is $\sim 50\%$ decrease in heart rate with only $\sim 1^\circ\text{C}$ decrease in T_b ; Milsom et al. 1999). The depressed torpid state is rapidly reversed upon arousals as well. Therefore, transitions into and out of torpor represent opportunities for profound ischemia/reperfusion injury. Ground squirrels also experience extremely low T_b 's and acidosis during torpor (van Breukelen et al. 2010). Each of these conditions alone is a well-characterized stressor that stimulates apoptosis when experienced in nonhibernating mammals. At the cellular level, hibernators experience a virtual block in homeostatic processes like transcription and translation during torpor (van Breukelen and Martin 2001, 2002b; van Breukelen et al. 2004). Presumably, these mismatches pose an energetic challenge during recovery to the interbout aroused (IBA) state. Execution of apoptosis is highly regulated and energetically expensive (Leist et al. 1997; Ferrari et al. 1998; Tatsumi et al. 2003; Skulachev 2006). Perhaps more importantly, these cells would need to be replenished during the IBA state when cellular turnover is possible (Wu and Storey 2012). Ground squirrels are anorexic for the entire hibernation season, meaning that such cell proliferation would have to come at the expense of seasonal energy stores and not from food (van Breukelen and Martin 2002a). Unmitigated and widespread apoptosis during the severely energy-limited hibernation season would be energetically costly and is at odds with both conserving energy and overall animal survival. Therefore, apoptosis is likely depressed in hibernating ground squirrels. However, little is known as to how this mitigation of apoptosis may be accomplished.

Apoptotic induction is dependent on the balance of the activities of many cellular regulators, including proapoptotic BCL-2 family members, such as BAD, BAX, and BAK; caspases; apoptosis-inducing factor; antiapoptotic BCL-2 family members, such as BCL-2 and BCL-XL; inhibitor of apoptosis proteins (IAPs); and kinases, such as Akt (Madrid et al. 2000; Philchenkov 2004; Czabotar et al. 2014). We chose to focus on the regulation of caspase 3 because of its role as the key executioner of apoptosis and because it is responsible for directly cleaving the bulk of the apoptotic substrates (Ramirez and Salvesen 2018). Caspase 3 is the convergence point for both extrinsic and intrinsic induction of apoptosis. The central role caspase 3 plays in integrating upstream apoptotic signals and then executing the apoptotic program makes it a critical target for understanding the fundamental nature of apoptotic signaling in cells. Caspase 3 is produced as an inactive zymogen, or procaspase. Activation is dependent on both intra-domain proteolytic cleavage (usually performed by other caspases) and large and small catalytic unit heterodimerization. Because of the dramatic structural changes associated with processing the 32-kDa (p32) procaspase 3 into the 17- and 12-kDa (p17 and p12) active fragments, caspase 3 activation results in extraordinary enzymatic activation. Liberation of p17 from procaspase 3 results in a $>10,000$ -fold increase in its ability to cleave target substrates (Boatright and Salvesen 2003). Examining upstream and downstream pathway components associated with caspase 3 allowed us to identify an incomplete signaling mechanism during hibernation. While there is some apparent activation of caspase 3, this seemingly spurious activation does not result in widespread apoptosis.

Methods

Animal Care and Tissue Collection

All tissue collection protocols were approved by the University of Nevada, Las Vegas, Institutional Animal Care and Use Committee. Adult golden-mantled ground squirrels (*Spermophilus [Callospermophilus] lateralis*) were captured during August from Kennedy Meadows, California, or Duck Creek, Utah. After transport to the laboratory at the University of Nevada, Las Vegas, some animals were immediately euthanized as a seasonal control group (summer active [SA]). To allow for precise determination of torpor status, the remaining squirrels were implanted with temperature-sensitive radiotelemeters as described previously (Mini Mitter VM-FH disc, Sun River, OR; Pan et al. 2014). By early November, telemeter-implanted squirrels were housed in an environmental chamber at 4°C to facilitate hibernation. We sampled ground squirrels from late January to February for IBA and torpid squirrels. Torpid animals had been torpid for a minimum of 3 d. The T_b of torpid squirrels was $\sim 5^\circ\text{C}$. All squirrels were euthanized by CO_2 asphyxiation except for the torpid and early-arousal animals, which were euthanized by decapitation because their low respiratory and heart rates preclude use of injectable or inhaled anesthetics. Squirrels were rapidly chilled on ice, and tissues (e.g., liver, heart, kidney, brain, gonads) were quickly snap-frozen in liquid nitrogen and stored at -80°C until use. Tissues were collected from animals in the summer (SA), while torpid, or while euthermic between torpor bouts (IBA). For terminal deoxynucleotidyl transferase-mediated deoxyuridine triphosphate nick-end labeling (TUNEL) assays, additional animals ($N = 3$ for each temperature) that were naturally arousing from torpor were sampled when core T_b 's were $9.97^\circ\text{C} \pm 0.07^\circ\text{C}$, $20.37^\circ\text{C} \pm 0.07^\circ\text{C}$, and $31.13^\circ\text{C} \pm 1.07^\circ\text{C}$ at the moment of sampling. Some assays included livers from rats as a nonhibernator comparison.

Sample Preparation and Western Blot Analyses

Livers were pulverized in liquid N_2 and homogenized in three volumes of 50 mM tris HCl, pH 8.3, 20% glycerol, 2% SDS, and 0.4 M β -mercaptoethanol using glass/glass homogenization. The homogenate was centrifuged at 20,000 g at 4°C for 30 min to remove cellular debris. Protein concentration of all supernatants was determined using a modified Lowry protein assay. For caspase 3, 70 μg of total protein from SA, torpid, and IBA squirrels ($N = 3$ for all states) was subjected to SDS-PAGE in 4%–20% gradient gels. Proteins were electrotransferred to PVDF membrane (400 mA for 3 h). Blots were blocked in 3% milk in 50 mM tris HCl, pH 8.0, 150 mM NaCl (TBS) with 0.5% Tween 20 (TBST) for 1 h. Incubation with a polyclonal primary antibody for caspase 3 (Santa Cruz Biotechnology, Santa Cruz, CA; rabbit polyclonal used at 1:300) was done overnight at 4°C . Washing between incubation steps consisted of one 5-min wash in TBS, followed by two 5-min washes in TBST and a final 5-min wash in TBS. Following washes, blots were exposed to HRP-conjugated secondary antibody (Amersham Biosciences, Amersham, UK) for 1 h in TBST with 1% BSA to block nonspecific binding. Visualization

was performed using ECL+ on a Typhoon imager (GE Health Sciences, Chicago, IL). For the inhibitor of caspase-activated deoxyribonuclease (ICAD) and poly (ADP-ribose) polymerase (PARP) analyses, 45 μ g of total protein from three squirrels in each metabolic state (SA, torpid, and IBA) were run on 17% (ICAD) or 14% (PARP) SDS-PAGE gels. The ICAD primary antibody was used at 1:1,000 (rabbit polyclonal; ProSci, Poway, CA), while the PARP primary antibody was used at 1:200 (rabbit polyclonal; Roche Diagnostics, Risch-Rotkreuz, Switzerland). Following washes, blots were exposed to IRDye 680LT-conjugated secondary antibodies (LiCor, Lincoln, NE; 1:10,000). ICAD and PARP blots were visualized on a LiCor Odyssey. All quantifications were performed in the linear range using either ImageQuant or LiCor software. Ponceau staining was performed to confirm equal loading of gel lanes.

Caspase 3 Activity Assays

Livers were pulverized in liquid N₂ and homogenized in one volume of 25 mM HEPES, pH 7.8, 5 mM EDTA, 0.1% CHAPS, 5 mM ATP, 10 mM DTT, 5 mM MgCl₂, and 10 mM KCl using glass/glass homogenization. The homogenate was centrifuged at 20,000 g and 4°C for 30 min to remove cellular debris. Protein concentration of all supernatants was determined using a modified Lowry assay. Caspase 3 reactions consisted of 20 mM HEPES, pH 7.6, 2 mM EDTA, 5 mM DTT, and either 500 μ g of protein (rat) or 1,000 μ g of protein (SA, torpid, IBA) in a total volume of 100 μ L. Assay mixtures were allowed to preincubate on ice for 30 min to reduce background. Reactions were initiated with the addition of 40 μ M DEVD-AMC (Sigma Chemical, St. Louis, MO; AMC indicates 7-amido 4-methylcoumarin). Following incubation at indicated temperatures and times, reactions were stopped with the addition of 10 μ L of concentrated HCl. Samples were centrifuged at 10,000 g for 12 min, and fluorescence was measured with excitation/emission spectra of 360/460 nm. Addition of 100 μ M Ac-DEVD-CHO, the specific competitive inhibitor of caspase 3, reduced activity to 26.6% \pm 4.6% ($N = 3$ for control and inhibited reaction; ANOVA, df = 5, $F = 173.5$, $P = 0.0002$) of the noninhibited rate. However, we found that assaying parallel reactions wherein HCl was added before substrate provided a more consistent basis for comparison, and all data are presented as such. Reactions were repeated for three different animals from each state with similar results. Linearity of the caspase 3 activity assay was measured in both rats and ground squirrels (data not shown; r^2 of linear fit was >0.99 and 0.96, respectively). Reaction incubation times are as indicated in figure legends (figs. 2, A1) and are within the linear range for both species. In these and our previous experiences with utilizing AMC-linked peptides as substrates, we found significant day-to-day variation in the extent of AMC cleavage (Velickovska et al. 2005). For that reason, we expressed all data as a percentage of maximum fluorescence within the assay to allow for direct comparison of different states.

TUNEL Assay

Caspase 3 activity results in the cleavage of ICAD (Sakahira et al. 1998). CAD moves into the nucleus and nicks DNA. As an indicator of downstream effects of caspase 3 activity, TUNEL

assays were performed to detect DNA nicking. Glass slides were dipped in 0.01% poly-L-lysine for 5 min and allowed to dry overnight before use. Tissues were embedded in Tissue-Tek OCT solution (Sakura Finetek USA, Torrance, CA) and frozen. Livers, kidneys, and hearts of ground squirrels from each metabolic state were used ($N = 3$ for each state: SA, torpid, IBA, and naturally arousing animals). Tissues were sectioned on a cryostat at 7 μ m thickness. Following application of the tissue slice to the slide, the slide was fixed in 4% paraformaldehyde for 20 min. Slides were washed three times for 5 min each in phosphate-buffered saline (PBS). Tissues were permeabilized for 5 min with 0.1% Triton X-100 before three washes for 5 min each in PBS. TUNEL reagent was added per manufacturer's instructions (Roche Diagnostics, Mannheim, Germany). Reactions were visualized on a confocal microscope. To ensure efficacy of the assay, some sections from each tissue were subjected to DNase treatment per the manufacturer's instructions. All TUNEL-positive cells were counted in each tissue slice. For an estimate of total cell numbers for each tissue slice, cells were counted in five separate fields, and the average cell count was multiplied by the number of fields per slice. The validity of this approach was confirmed by counting all cells on some representative tissue slices.

Most of the work presented here used liver, as much of our earlier data on the control of transcription, translation, and protein degradation focuses on this tissue (van Breukelen and Martin 2001, 2002b; van Breukelen and Carey 2002; van Breukelen et al. 2004; Velickovska et al. 2005; Velickovska and van Breukelen 2007; Pan et al. 2014). To ensure that liver was representative of other tissues, TUNEL assays were performed on heart and kidney as well.

Statistical Analysis

Data are presented as mean \pm standard error. Where assumptions of normality were met, statistical analyses were performed using ANOVA with Fisher's least significant difference post hoc analysis for specific comparisons (ANOVAs were performed using KaleidaGraph ver. 4.5 for Mac; Synergy Software, Reading, PA). Statistical significance was assumed when $P < 0.05$.

Results

Caspase 3 activation occurs when the p32 proenzyme is cleaved to form the active caspase p17 and p12 fragments (Han et al. 1997). Using Western blotting, we resolved three bands representing the p32 proenzyme, a p20 intermediate form, and the most active p17 fragment, as confirmed by migration of the bands with respect to the molecular weight standard (fig. 1B). Caspase 3 appears activated in both torpid and IBA winter animals, as evidenced by an approximately twofold increase in p17 concentrations compared with SA squirrels (fig. 1; ANOVA, $P < 0.05$). For simplicity, only the most active caspase fragment is shown in figure 1B, and data are normalized to the SA state, although all data are available in table A1.

Liberation of p17 typically signifies caspase 3 activation. Western blot data do not address actual enzymatic activity per se. Therefore, we directly examined the catalytic activity of

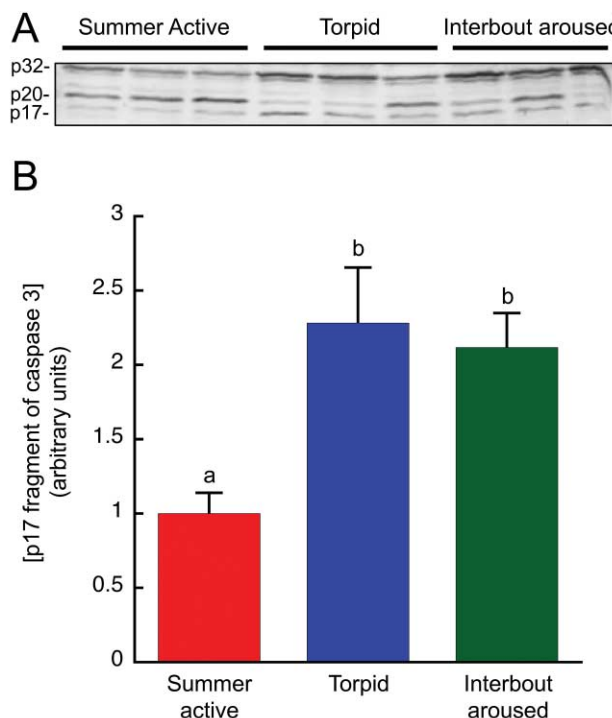


Figure 1. Concentration of the most catalytically active p17 fragment of caspase 3 is increased ~2-fold in winter squirrels. Ground squirrel livers ($N = 3$ animals per state) were obtained in the summer (summer active) and during hibernation when animals were torpid or between bouts of torpor (interbout aroused). Caspase activation occurs in a step-wise activation cascade where the 32-kDa pro-caspase 3 (p32) is cleaved to form the p20 fragment. Further cleavage of p20 produces the fully active p17 and p12 fragments. *A*, Caspase 3 Western blot resolved three caspase 3 bands: p32 pro-caspase (top band), p20 intermediate fragment (middle band), and the fully active p17 fragment (bottom band). The p12 fragment was not recognized by our antibody. *B*, Summarized data for caspase 3 p17 fragment. The graph shows mean \pm SE. Different lower-case letters denote significant differences (ANOVA, $P < 0.05$).

caspase 3 (fig. 2). Although the low assay temperatures typical of torpor (e.g., 0°C–10°C) resulted in a predictable depression in caspase 3 activity, there was still measurable activity even at 0°C in all ground squirrel states (SA, torpid, and IBA) and even in rats. Figure 2 depicts the results of individual animals, but similar data were obtained for an additional two animals per state (data not shown). Background fluorescence represents a greater proportion of maximum rate in torpid hibernating squirrels than in other groups, suggesting less total activity (fig. 2C), although the capacitance data do not reveal significant differences (fig. A1). The capacitance data were generated by conducting simultaneous assays using 1 mg of protein from $N = 3$ animals for each state and measured at 30°C. This approach allowed us to avoid the issues with day-to-day variation in the extent of AMC cleavage and directly compare animals in different states. Had there been a bona fide 10,000-fold activation, one might expect fluorometer saturation even for the cold temperature assays. Interestingly, caspase 3 activity was markedly and

specifically depressed at an assay temperature of 37°C in winter squirrels (torpid and IBA; ANOVA, $df = 8, F = 15.31, P = 0.0044$) but not in SA squirrels or rats. Activity at 37°C was depressed 34.85% \pm 8.39% of the rate at 30°C for IBA animals and 32.33% \pm 14.76% for torpid animals ($N = 3$ different animals). A Western blot for caspase 3 in an IBA lysate incubated at 0°C, 20°C, and 37°C and sampled at four time points revealed no evidence for in vitro caspase 3 degradation during the incubation (data not shown; ANOVA, $df = 11, F = 1.319, P = 0.3145$).

Activated caspase 3 cleaves cellular targets such as ICAD and PARP (Fischer et al. 2003). We found no changes in ICAD (fig. 3A) or PARP (fig. 3B) cleavage products as a function of state (ANOVA: for ICAD, $df = 8, F = 1.435, P = 0.3095$; for PARP, $df = 8, F = 1.246, P = 0.3527$).

TUNEL activity was remarkably low in all states for all tissues (fig. 4; table 1). We verified the assay by treating some slides with DNase as a positive control (fig. 4B). Further verification of the TUNEL assay using rat livers demonstrated much higher levels (~15 times) of TUNEL-positive cells (data not shown). To address whether there was an increase in DNA nicking activity as animals aroused from torpor that would have ceased by the time animals completed arousing (i.e., in IBA squirrels), we sampled livers from squirrels at 10°C, 20°C, and 30°C during natural arousals (table 2). We found no evidence for widespread TUNEL activity.

Discussion

Hibernators experience numerous conditions that are known to be proapoptotic in nonhibernators. However, widespread apoptosis is at odds with the energetic savings associated with hibernation. Survival of hibernation presumably depends on mitigating apoptosis. Several studies in hibernators examined pro- and antiapoptotic regulators, such as the BCL family members and IAPs (Cai et al. 2004; Fleck and Carey 2005; Kurtz et al. 2006; Mele et al. 2015; Fu et al. 2016). These studies have not revealed a pervasive antiapoptotic system. Although Western blot analyses for six key proteins, such as BCL-2 and XIAP, suggested a coordinated and widespread antiapoptotic program in heart and brain of hibernating 13-lined ground squirrels (*Spermophilus* [*Ictidomys*] *tridecemlineatus*), other tissues, such as kidney, liver, and brown adipose tissue, exhibited reduced availability of some of these antiapoptotic factors (Roule et al. 2013). Cellular signaling also shows mixed results. For example, while Akt was phosphorylated in the brains of greater horseshoe bats (*Rhinolophus ferrumequinum*) arousing from hibernation, suggesting an inhibition of apoptotic signaling (Lee et al. 2002), in a study of hibernating little brown bats (*Myotis lucifugus*), availability and phosphorylation status of Akt were variable depending on tissue type and torpor status (e.g., brain vs. heart; Eddy and Storey 2003). If mitigation of widespread apoptosis is being effected through described antiapoptotic mechanisms, one might expect a more coordinated approach common to all tissues and reflective of the need to suppress apoptosis in both torpid and aroused animals, since these animals are anorexic for the entire winter (van Breukelen and Martin 2002b).

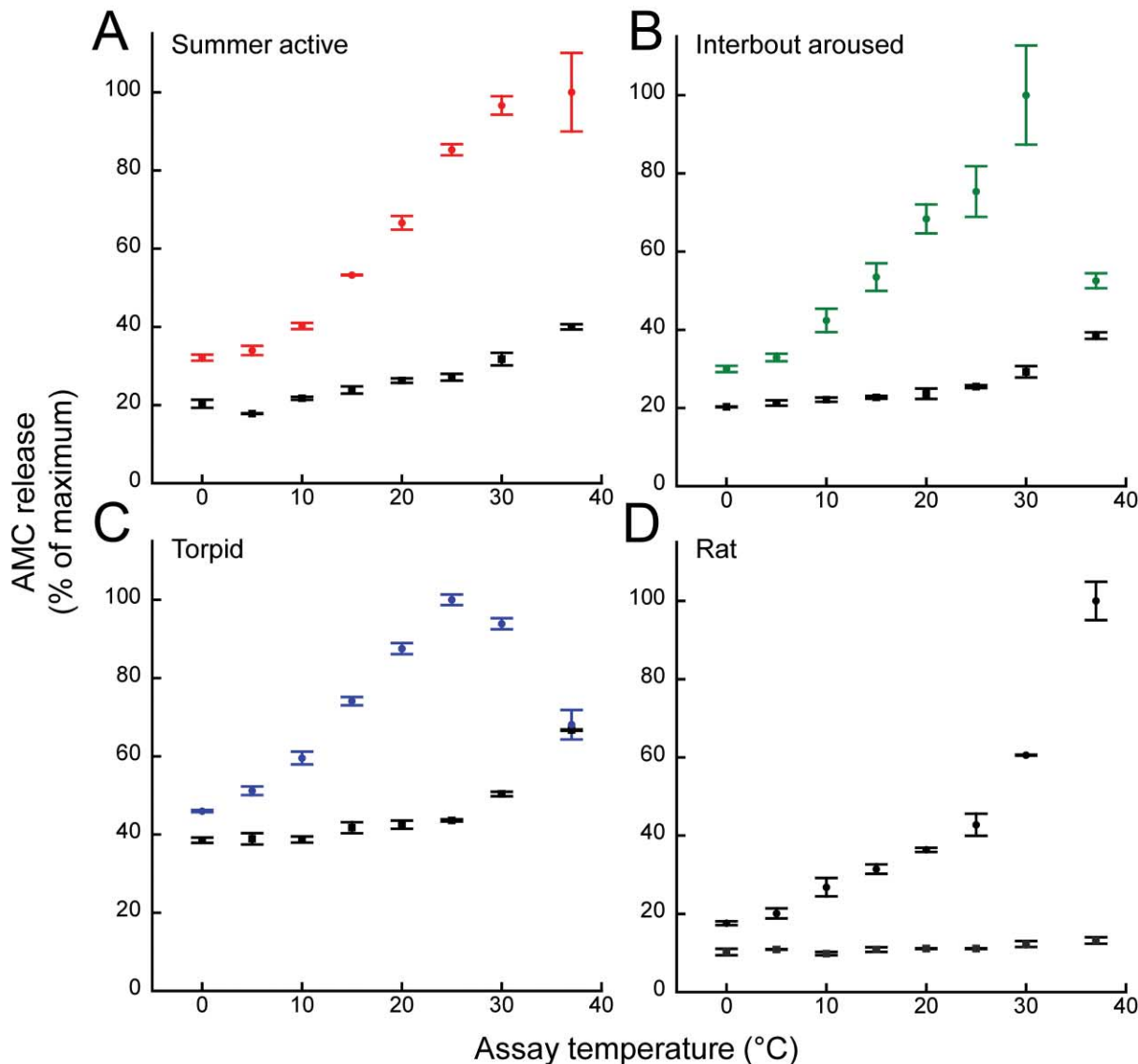


Figure 2. Caspase 3 enzymatic activity as a function of assay temperature. Values are mean \pm SE for three samples of a control lysate (quenched reactions for evaluation of background fluorescence, squares) and three samples of the same lysate that was not inhibited (circles) from a representative animal from summer active (A), interbout aroused (B), and torpid (C) states and from a rat (D) for nonhibernator comparison. Similar results were obtained using $N = 3$ animals from each state. AMC = 7-amido 4-methylcoumarin.

Here, we chose to focus our attention on the regulation of caspase 3, with the rationale that as the key executioner caspase, it is required to directly cleave numerous critical substrates leading to apoptosis. Therefore, the activation status of caspase 3 and associated events can clarify whether hibernators are experiencing apoptotic signaling leading to widespread apoptosis during hibernation. We assayed for indications of caspase 3 activation, *in vitro* proteolytic activity, and caspase 3-mediated downstream events in hibernating ground squirrels compared with SA controls. We found a twofold increase in the p17 fragment of caspase 3 during winter (fig. 1). This level of p17 liberation is expected to increase enzymatic activity of caspase 3 by $>10,000$ -fold (Boatright and Salvesen 2003). However, enzymatic activity assays re-

vealed no dramatic increases in activity during winter regardless of assay temperature (fig. 2). Furthermore, examination of downstream targets of caspase 3 indicated no increased cleavage of ICAD, PARP, or DNA nicking consistent with apoptosis (figs. 3, 4). The apparent caspase 3 activation did not result in widespread apoptosis during hibernation.

Caspase 3 activation is thought to occur in an all-or-none fashion (Rehm et al. 2002). When one considers that a Western blot represents the average protein signal from a large number of cells, one should expect almost undetectable caspase 3 activation when relatively few cells are undergoing apoptotic signaling. Our ability to detect a twofold liberation of p17 (fig. 1) suggests that caspase 3 was modestly activated in a large proportion of cells

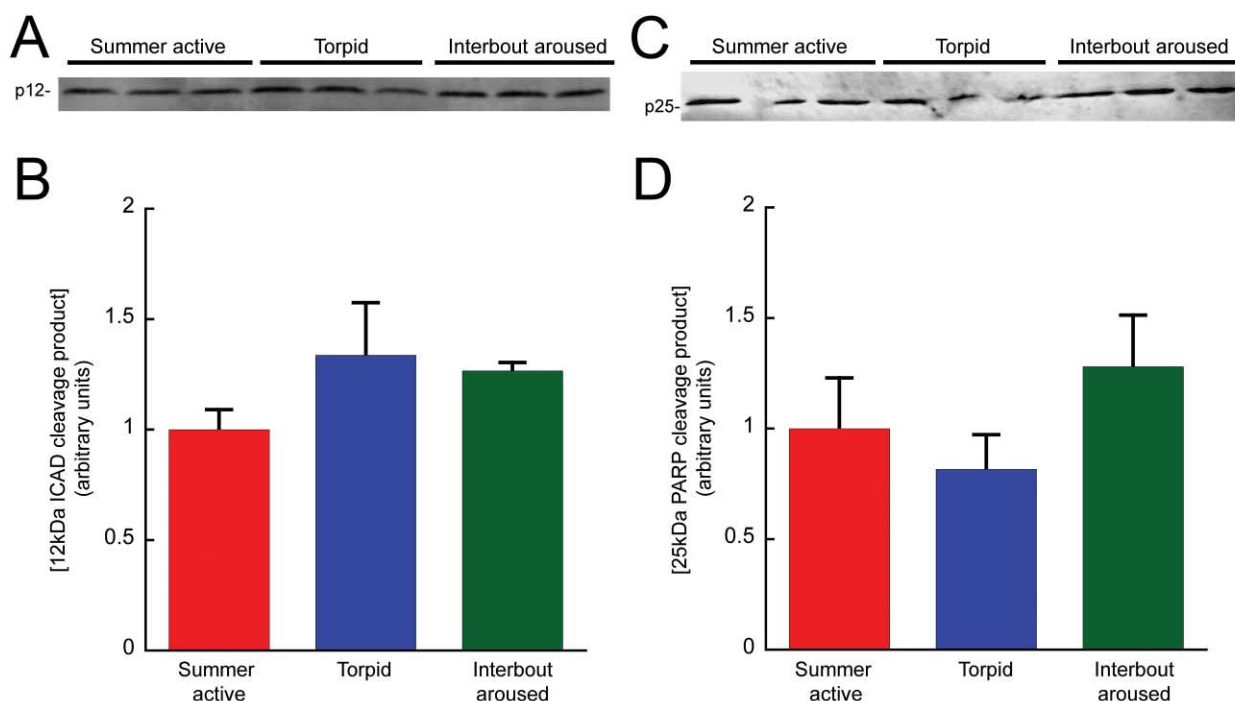


Figure 3. Cleavage of caspase 3 targets inhibitor of caspase-activated deoxyribonuclease (ICAD) and poly (ADP-ribose) polymerase (PARP) as a function of metabolic state suggests little bona fide activity of caspase 3. *A*, Western blot for p12 of the ICAD in liver lysates from $N = 3$ animals representing summer active, interbout aroused, and torpid states. *B*, Summary data show mean \pm SE for the 12-kDa ICAD cleavage product. *C*, Western blot for p25 of the PARP. *D*, Summary data show mean \pm SE for the 25-kDa PARP cleavage product. No statistical differences were found in cleavage products as a function of state (ANOVA, $P > 0.05$).

(e.g., to accomplish a twofold increase in p17 availability, one would expect either a large number of cells to undergo apoptosis or that there was a modest graded type of response in many cells). The graded response of modest activation in many cells is more consistent with our TUNEL data (table 1). As discussed below,

we contend that this seeming activation of caspase 3 in our study may simply be a spurious consequence of poor regulation.

The seeming and widespread activation of caspase 3 should have resulted in dramatic increases in enzymatic activity measured through cleavage of the artificial substrate DEVD-AMC.

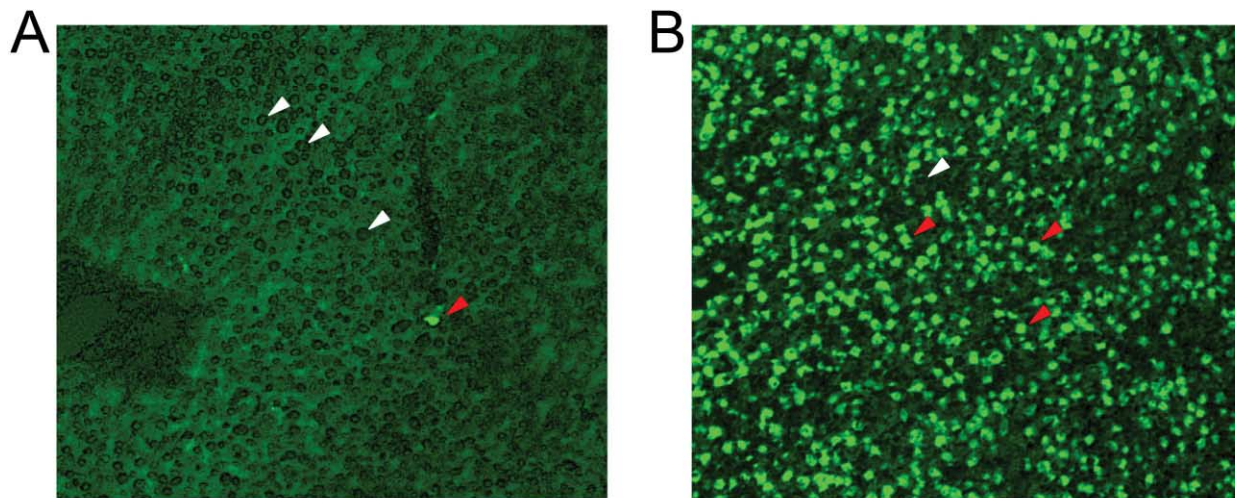


Figure 4. Apoptosis is extremely limited regardless of state. *A*, Representative results of terminal deoxynucleotidyl transferase-mediated deoxyuridine triphosphate nick-end labeling (TUNEL) assays for the detection of nicked DNA in 7- μ m liver slices. *B*, DNase-treated liver slice showing widespread apoptotic activation. Apoptotic nuclei are indicated by red arrowheads, while nonapoptotic nuclei are indicated by white arrowheads.

Table 1: Results of TUNEL assay for DNA nicking in ground squirrel tissues

Tissue, state	TUNEL-positive nuclei slide ⁻¹	Estimated nuclei counted	TUNEL positive (%)
Liver:			
Summer active	2.00 ± .58	74,636 ± 10,389	3.01 × 10 ⁻³ ± 1.03 × 10 ⁻³
Torpid	.67 ± .33	45,462 ± 7,405	1.73 × 10 ⁻³ ± 9.45 × 10 ⁻⁴
Interbout aroused	.33 ± .33	35,051 ± 7,334	1.41 × 10 ⁻³ ± 1.41 × 10 ⁻³
Heart:			
Summer active	.67 ± .33	18,183 ± 1,286	3.70 × 10 ⁻³ ± 1.89 × 10 ⁻³
Torpid	.67 ± .33	27,864 ± 9,257	2.27 × 10 ⁻³ ± 1.34 × 10 ⁻³
Interbout aroused	.67 ± .67	12,890 ± 2,192	7.76 × 10 ⁻³ ± 7.76 × 10 ⁻³
Kidney:			
Summer active	.33 ± .33	138,053 ± 29,343	2.76 × 10 ⁻⁴ ± 2.76 × 10 ⁻⁴
Torpid	2.00 ± 1.00	120,526 ± 25,337	2.13 × 10 ⁻³ ± 1.12 × 10 ⁻³
Interbout aroused	2.33 ± 1.45	121,527 ± 155,572	1.72 × 10 ⁻³ ± 1.08 × 10 ⁻³

Note. Data are mean ± SE for $N = 3$ animals for each state and tissue. There are no statistical differences (ANOVA, $P > 0.05$). TUNEL = terminal deoxynucleotidyl transferase-mediated deoxyuridine triphosphate nick-end labeling.

Our data do not support that expectation (fig. 2). Despite an expectation of >10,000-fold more activity, the activity of winter lysates was comparable to that of summer lysates. Indeed, the increased background seen in torpid animal lysates suggests depressed activity, although capacitance data reveal no differences (fig. A1).

We found that caspase 3 activity in both torpid and IBA squirrels was markedly and specifically depressed by ~2/3 at 37°C (fig. 2B, 2C). We initially interpreted this depression as a bona fide regulatory event to depress apoptosis during IBA periods. However, heterologous assays wherein torpid lysates were added to rat lysates revealed no depression of enzymatic activity, suggesting that there was no hibernation-specific inhibitor (fig. A2). Additionally, we see a similar depression at 37°C was present for other caspases even in most SA squirrel lysates (Treat et al. 2023). In other words, the effect is not specific to caspase 3 or even to hibernating ground squirrels. We contend that the effect likely represents an artifact of a lengthy assay as opposed to a legitimate caspase 3-specific regulatory event.

The expected downstream effects of active caspase 3 include the cleavage of ICAD and PARP resulting in DNA nicking (Fischer et al. 2003). ICAD and PARP were not cleaved during hibernation (fig. 3). Our results agree with those for white adipose tissue in *S. tridecemlineatus*, wherein PARP cleavage did not change with hibernation state (Logan et al. 2016). Our TUNEL assays in liver, heart, and kidney tissues reveal no widespread DNA nicking during hibernation in multiple tissues (table 1). Apoptotic execution can occur in as little as 1 h, and arousal from torpor can occur in as little as 2–3 h (Tyas et al. 2000; Utz et al. 2007). Our inclusion of arousing animals at three well-defined points during the arousal process in which there was also little to no TUNEL activity precludes our missing of rapidly executed apoptotic events during arousals (table 2). Furthermore, we noted remarkably little TUNEL activity in both active states (IBA and SA) compared with rats, which may suggest a species- or hibernator-specific depression of apoptosis.

Importantly, our data allow for a better understanding of the conflicting extant data on mitigation of apoptosis during

Table 2: Results of TUNEL assay for DNA nicking in tissues of ground squirrels arousing from torpor

Tissue, T_b at time of sampling (°C)	TUNEL-positive nuclei slide ⁻¹	Estimated nuclei counted	TUNEL positive (%)
Liver:			
10	1.00 ± 1.00	52,379 ± 13,330	3.24 × 10 ⁻³ ± 3.24 × 10 ⁻³
20	2.67 ± 2.19	53,805 ± 12,624	8.56 × 10 ⁻³ ± 7.76 × 10 ⁻³
30	1.33 ± 1.33	788,998 ± 14,491	1.40 × 10 ⁻³ ± 1.40 × 10 ⁻³
Heart:			
10	.33 ± .33	18,694 ± 3,114	2.52 × 10 ⁻³ ± 2.52 × 10 ⁻³
20	.67 ± .67	19,754 ± 4,055	2.43 × 10 ⁻³ ± 2.43 × 10 ⁻³
30	1.00 ± .57	20,097 ± 3,024	5.35 × 10 ⁻³ ± 2.73 × 10 ⁻³
Kidney:			
10	4.00 ± 2.08	101,399 ± 23,188	4.17 × 10 ⁻³ ± 2.43 × 10 ⁻³
20	4.00 ± 2.31	103,877 ± 15,314	4.67 × 10 ⁻³ ± 2.89 × 10 ⁻³
30	3.67 ± 1.20	57,428 ± 12,719	6.11 × 10 ⁻³ ± 6.57 × 10 ⁻⁴

Note. Data are mean ± SE for $N = 3$ animals for each temperature and tissue. There are no statistical differences (ANOVA, $P > 0.05$). TUNEL = terminal deoxynucleotidyl transferase-mediated deoxyuridine triphosphate nick-end labeling.

hibernation. For instance, data from white adipose tissue in *S. tridecemlineatus* demonstrated cleaved caspase 3 was lowest in early torpor (torpid for ~1 d) but was increased during early arousal and interbout arousal (Logan et al. 2016). Earlier work compared the enzymatic activity of caspase 3 in lysates at one or two temperatures and found conflicting results: ~35% decrease in caspase 3 activity in intestine but ~36% increase in caspase 3 activity in kidney for IBA squirrels (Fleck and Carey 2005; Jani et al. 2011). By exploiting a systems-level approach, we avail ourselves of multiple lines of evidence to demonstrate no widespread apoptosis during hibernation. Had earlier studies incorporated both upstream and downstream indicators of the executors of apoptosis, the mitigation of apoptosis during hibernation might have been made clearer.

An appropriate question is, Why would there be activation of caspase 3 without the downstream events (e.g., the incomplete signaling of apoptosis)? A simple answer could be that squirrels are unable to prevent this activation but instead are able to mitigate apoptosis further downstream in the pathway. The non-steady-state condition of torpor may simply not allow for regulation mechanisms common in steady-state conditions. Other examples of this lack of coordination due to the non-steady-state conditions are available. During protein degradation, the process of ubiquitylation is much less temperature sensitive than proteolysis *per se* (van Breukelen and Carey 2002; Velickovska et al. 2005; Velickovska and van Breukelen 2007). The result of continued ubiquitylation without degradation is an accumulation of ubiquitin conjugates during torpor. Similarly, p53 function does not result in anticipated changes in gene expression despite its entering the nucleus during torpor, binding to DNA, and recruiting RNA polymerase II (Pan et al. 2014). The steady-state assumptions of homeostatic mechanisms are inappropriate in the non-steady-state condition of torpor. Investigations of hibernation require a thoughtful systems-level approach that incorporates upstream and downstream events when possible (van Breukelen 2016).

Taken together, our data demonstrate mitigation of apoptosis during hibernation. Importantly, the mechanism is not simply avoidance of all caspase recruitment or activation. Instead, there is seeming caspase 3 activation that is not fully translated into the execution of an apoptotic event. These data suggest that there may be more flexibility in apoptotic signaling even after canonical points of no return like caspase 3 activation. We recognize that our data do not address a specific mechanism that inhibits caspase 3 activity. However, global regulation of caspases during hibernation may be affected by ubiquitylation. As mentioned previously, an inability to depress ubiquitylation results in a two- to threefold accumulation of ubiquitin conjugates during torpor (van Breukelen and Carey 2002). Ubiquitylation of caspase 3 is known to inhibit caspase 3 proteolytic activity independent of caspase 3 degradation (Ditzel et al. 2008; Schile et al. 2008; Bader and Steller 2009). Unfortunately, we are unaware of an experimental approach that would allow us to directly address this mechanism in a hibernator at this time. Finally, our understanding of how cells avoid apoptosis is evolving. For instance, in the recently described process of anastasis, cells have been able to

recover from canonical points of no return, such as caspase 3 activation, DNA damage, and even apoptotic body formation (Tang and Tang 2018). We are hopeful that lessons learned from further elucidation of anastasis and similar mechanisms may be applied toward understanding how hibernators avoid apoptosis despite the activation of caspase 3.

Acknowledgments

The laboratory is supported by the National Science Foundation (IOS-1655091). We thank members of the laboratory and, in particular, Bryan Lloyd for assistance with experiments and animal care. All applicable international, national, and/or institutional guidelines for the care and use of animals were followed. All procedures in studies involving animals were performed in accordance with the ethical standards of the institution or practice where the studies were conducted.

Literature Cited

Andrews M.T. 2019. Molecular interactions underpinning the phenotype of hibernation in mammals. *J Exp Biol* 222: jeb160606. <https://doi.org/10.1242/jeb.160606>.

Bader M. and H. Steller. 2009. Regulation of cell death by the ubiquitin-proteasome system. *Curr Opin Cell Biol* 21:878–884.

Barnes B.M. 1989. Freeze avoidance in a mammal: body temperatures below 0°C in an Arctic hibernator. *Science* 24: 1593–1595.

Boatright K.M. and G.S. Salvesen. 2003. Caspase activation. *Biochem Soc Symp* 70:233–242.

Cai D., R.M. McCarron, Z.Y. Erik, Y. Li, and J. Hallenbeck. 2004. Akt phosphorylation and kinase activity are down-regulated during hibernation in the 13-lined ground squirrel. *Brain Res* 1014:14–21.

Czabotar P.E., G. Lessene, A. Strasser, and J.M. Adams. 2014. Control of apoptosis by the BCL-2 protein family: implications for physiology and therapy. *Nat Rev Mol Cell Biol* 15:49.

Ditzel M., M. Broemer, T. Tenev, C. Bolduc, T.V. Lee, K.T.G. Rigbolt, R. Elliot, et al. 2008. Inactivation of effector caspases through nondegradative polyubiquitylation. *Mol Cell* 32:540–553.

Eddy S.F. and K.B. Storey. 2003. Differential expression of Akt, PPAR γ , and PGC-1 during hibernation in bats. *Biochem Cell Biol* 81:269–274.

Ferrari D., A. Stepczynska, M. Los, S. Wesselborg, and K. Schulze-Osthoff. 1998. Differential regulation and ATP requirement for caspase-8 and caspase-3 activation during CD95- and anticancer drug-induced apoptosis. *J Exp Med* 188:979–984.

Fischer U., R.U. Janicke, and K. Schulze-Osthoff. 2003. Many cuts to ruin: a comprehensive update of caspase substrates. *Cell Death Differ* 10:76.

Fleck C.C. and H.V. Carey. 2005. Modulation of apoptotic pathways in intestinal mucosa during hibernation. *Am J Physiol* 289:R586–R595.

Fu W., H. Hu, K. Dang, H. Chang, B. Du, X. Wu, and Y. Gao. 2016. Remarkable preservation of Ca^{2+} homeostasis and inhibition of apoptosis contribute to anti-muscle atrophy effect in hibernating Daurian ground squirrels. *Sci Rep* 6: 27020.

Geiser F. 2021. Ecological physiology of daily torpor and hibernation. Springer, Cham, Switzerland.

Han Z., E.A. Hendrickson, T.A. Bremner, and J.H. Wyche. 1997. A sequential two-step mechanism for the production of the mature p17: p12 form of caspase-3 in vitro. *J Biol Chem* 272:13432–13436.

Jani A., E. Epperson, J. Martin, A. Pacic, D. Ljubanovic, S.L. Martin, and C.L. Edelstein. 2011. Renal protection from prolonged cold ischemia and warm reperfusion in hibernating squirrels. *Transplantation* 92:1215–1221.

Kurtz C.C., S.L. Lindell, M.J. Mangino, and H.V. Carey. 2006. Hibernation confers resistance to intestinal ischemia-reperfusion injury. *Am J Physiol* 291:G895–G901.

Lee M., I. Choi, and K. Park. 2002. Activation of stress signaling molecules in bat brain during arousal from hibernation. *J Neurochem* 82:867–873.

Leist M., B. Single, A.F. Castoldi, S. Kühnle, and P. Nicotera. 1997. Intracellular adenosine triphosphate (ATP) concentration: a switch in the decision between apoptosis and necrosis. *J Exp Med* 185:1481–1486.

Logan S.M., B.E. Luu, and K.B. Storey. 2016. Turn down genes for WAT? activation of anti-apoptosis pathways protects white adipose tissue in metabolically depressed thirteen-lined ground squirrels. *Mol Cell Biochem* 416:47–62.

Madrid L.V., C.Y. Wang, D.C. Guttridge, A.J. Schottelius, A.S. Baldwin, and M.W. Mayo. 2000. Akt suppresses apoptosis by stimulating the transactivation potential of the RelA/p65 subunit of NF- κ B. *Mol Cell Biol* 20:1626–1638.

Mele M., R. Alo, E. Avolio, and M. Canonaco. 2015. Bcl-2/Bax expression levels tend to influence AMPAergic trafficking mechanisms during hibernation in *Mesocricetus auratus*. *J Mol Neurosci* 55:374–384.

Milsom W.K., M.B. Zimmer, and M.B. Harris. 1999. Regulation of cardiac rhythm in hibernating mammals. *Comp Biochem Physiol A* 124:383–391.

Pan P., M.D. Treat, and F. van Breukelen. 2014. A systems-level approach to understanding transcriptional regulation by p53 during mammalian hibernation. *J Exp Biol* 217: 2489–2498.

Philchenkov A. 2004. Caspases: potential targets for regulating cell death. *J Cell Mol Med* 8:432–444.

Ramirez M.L.G. and G.S. Salvesen. 2018. A primer on caspase mechanisms. *Semin Cell Dev Biol* 82:79–85.

Rehm M., H. Dussmann, R.U. Janicke, J.M. Tavare, D. Kogel, and J.H. Prehn. 2002. Single-cell fluorescence resonance energy transfer analysis demonstrates that caspase activation during apoptosis is a rapid process: role of caspase-3. *J Biol Chem* 277:24506–24514.

Rouble A.N., J. Hefler, H. Mamady, K.B. Storey, and S.N. Tessier. 2013. Anti-apoptotic signaling as a cytoprotective mechanism in mammalian hibernation. *Peer J* 1:e29.

Sakahira H., M. Enari, and S. Nagata. 1998. Cleavage of CAD inhibitor in CAD activation and DNA degradation during apoptosis. *Nature* 391:96.

Schile A.J., M. Garcia-Fernandez, and H. Steller. 2008. Regulation of apoptosis by XIAP ubiquitin-ligase activity. *Genes Dev* 22:2256–2266.

Sherman P.W. and M.L. Morton. 1984. Demography of Belding's ground squirrels. *Ecology* 65:1617–1628.

Skulachev V.P. 2006. Bioenergetic aspects of apoptosis, necrosis and mitoptosis. *Apoptosis* 11:473–485.

Tang H.M. and H.L. Tang. 2018. Anastasis: recovery from the brink of cell death. *R Soc Open Sci* 5:180442.

Tatsumi T., J. Shiraishi, N. Keira, K. Akashi, A. Mano, S. Yamanaka, S. Matoba, S. Fushiki, H. Fliss, and M. Nakagawa. 2003. Intracellular ATP is required for mitochondrial apoptotic pathways in isolated hypoxic rat cardiac myocytes. *Cardiovasc Res* 59: 428–440.

Treat M. A.J. Marlon, L. Samentar, N. Caberoy, and F. van Breukelen. 2023. Mitigating apoptotic and inflammatory signaling via global caspase inhibition in hibernating ground squirrels, *Spermophilus lateralis*. *Physiol Biochem Zool* 96:53–61.

Tyas L., V.A. Brophy, A. Pope, A.J. Rivett, and J.M. Tavare. 2000. Rapid caspase 3 activation during apoptosis revealed using fluorescence resonance energy transfer. *EMBO Rep* 1: 266–270.

Utz J.C., V. Velickovska, A. Shmereva, and F. van Breukelen. 2007. Temporal and temperature effects on the maximum rate of rewarming from hibernation. *J Therm Biol* 32:276–281.

van Breukelen F. 2016. Applying systems-level approaches to elucidate regulatory function during mammalian hibernation. *Temperature* 3:524–526.

van Breukelen F. and H. Carey. 2002. Ubiquitin conjugate dynamics in the gut and liver of hibernating ground squirrels. *J Comp Physiol B* 172:269–273.

van Breukelen F., G. Krumschnabel, and J.E. Podrabsky. 2010. Vertebrate cell death in energy-limited conditions and how to avoid it: what we might learn from mammalian hibernators and other stress-tolerant vertebrates. *Apoptosis* 15:386–399.

van Breukelen F. and S.L. Martin. 2001. Translational initiation is uncoupled from elongation at 18°C during mammalian hibernation. *Am J Physiol* 281:R1374–R1379.

———. 2002a. Molecular adaptations in mammalian hibernators: unique adaptations or generalized responses? *J Appl Physiol* 92:2640–2647.

———. 2002b. Reversible depression of transcription during hibernation. *J Comp Physiol B* 172:355–361.

———. 2015. The hibernation continuum: physiological and molecular aspects of metabolic plasticity in mammals. *Physiology* 30:273–281.

van Breukelen F., P. Pan, C.M. Rausch, J.C. Utz, and V. Velickovska. 2008. Homeostasis on hold: implications of imprecise

coordination of protein metabolism during mammalian hibernation. Pp. 163–170 in B. Lovegrove and A. McKechnie, eds. Hypometabolism in animals: hibernation, torpor and cryobiology. Interpak, Pietermaritzburg, South Africa.

van Breukelen F., N. Sonenberg, and S.L. Martin. 2004. Seasonal and state-dependent changes of eIF4E and 4E-BP1 during mammalian hibernation: implications for the control of translation during torpor. *Am J Physiol* 287:R349–R353.

Velickovska V., B.P. Lloyd, S. Qureshi, and F. van Breukelen. 2005. Proteolysis is depressed during torpor in hibernators at the level of the 20S core protease. *J Comp Physiol B* 175:329–335.

Velickovska V. and F. van Breukelen. 2007. Ubiquitylation of proteins in livers of hibernating golden-mantled ground squirrels, *Spermophilus lateralis*. *Cryobiology* 55:230–235.

Wang L.C. and T.F. Lee. 1996. Torpor and hibernation in mammals: metabolic, physiological, and biochemical adaptations. *Compr Physiol* 14(suppl.):507–532.

Wu C.W. and K.B. Storey. 2012. Pattern of cellular quiescence over the hibernation cycle in liver of thirteen-lined ground squirrels. *Cell Cycle* 11:1714–1726.